

Zeolitic Imidazolate-Zinc MOF: An Eco-Friendly Heterogeneous Catalyst for Efficient Chromenes Synthesis and Conformational Analysis

**Ashraf Sadat Shahvelayati^{1,2*}, Jamshid Najafpour^{1,2}, Shabnam Alibakhshi¹,
Shabnam Sheshmani^{1,2}, Leila Hajiaghababaei^{1,2}**

¹*Department of Chemistry, Yadegar-e-Imam Khomeini (RAH) Shahre Ray Branch, Islamic Azad University, Tehran, Iran*

²*Research Center for New Technologies in Chemistry and Related Sciences, Yadegar-e-Imam Khomeini (RAH) Shahre Rey Branch, Islamic Azad University, Tehran, Iran*

(Received 10 May 2024; Final revised received 17 Aug. 2024)

Abstract

An effective synthesis technique for chromenes is presented, encompassing the reaction between hydroxynaphthoquinone, aryl aldehydes, and 4-coumarinol, using zeolitic imidazolate framework (ZIF-8) as an efficient catalyst, all without the need for solvents. Various parameters were optimized, including temperature, catalyst quantity, and reaction duration. The experiment was conducted using different solvents, with optimal results obtained in a solvent-free environment. This innovative method offers several advantages, including mild reaction conditions, a short reaction time (15-30 minutes), straightforward work-up, and impressive yields (88-98%) of biologically active products. Notably, this approach eliminates the reliance on hazardous solvents. Additionally, the conformational analysis of some synthesized chromenes was studied using thermodynamic properties through DFT calculations in the gas phase and DMSO solvent.

Keywords: Chromenes, Metal-organic framework (MOF), Multi-components Solvent-free reactions, ZIF-8, The conformational analysis.

***Corresponding author:** Ashraf Sadat Shahvelayati, Department of Chemistry, Yadegar-e-Imam Khomeini (RAH) Shahre Ray Branch, Islamic Azad University, Tehran, Iran and Research Center for New Technologies in Chemistry and Related Sciences, Yadegar-e-Imam Khomeini (RAH) Shahre Rey Branch, Islamic Azad University, Tehran, Iran. Email: avelayati@yahoo.com, a_shahvelayati@iau.ir.

Introduction

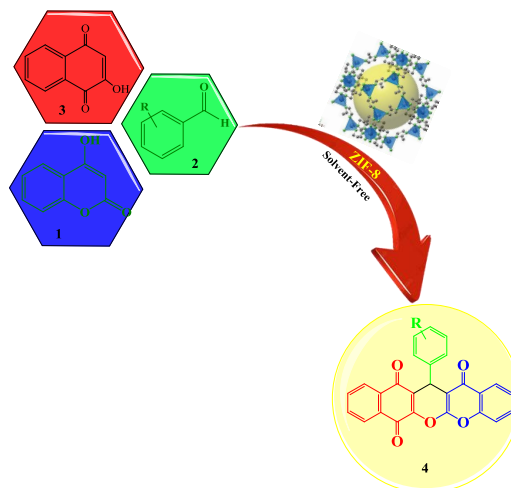
The multi-component reaction (MCR) has gained considerable attention as a versatile synthetic approach in the production of pharmaceuticals and industrial chemicals [1]. These reactions contribute to ecologically sustainable processes by minimizing waste, the consumption of energy, and the total count of reaction stages [2]. Among the various classes of heterocyclic molecules, oxygen heterocycles, particularly chromene heterocycles, are noteworthy due to their abundant natural availability and wide-ranging biological and pharmacological significance. Chromene heterocycles have demonstrated diverse biological activities, including antimicrobial, antimalarial, antiviral, and anticancer properties, making them valuable in sectors such as cosmetics, pigments, and biodegradable agrochemicals [3-9].

Several reagents and catalysts have been documented for the synthesis of chromene derivatives, including nanoparticles of clinoptilolite impregnated with potassium fluoride (KF/CP NPs) [10], Basic $\text{Fe}_3\text{O}_4@\text{C}$ nanocatalyst [11], $\text{ZnAl}_2\text{O}_4\text{-Bi}_2\text{O}_3$ nanopowder [12], $\text{ZnS}/\text{CuFe}_2\text{O}_4/\text{agar}$ organometallic hybrid catalyst [13], and the magnetic $\text{CaMgFe}_2\text{O}_4$ base nanocatalyst [14]. Other notable catalysts include $\gamma\text{-Fe}_2\text{O}_3@\text{SiO}_2\text{-SCH}_2\text{CO}_2\text{H}$ [15], $\text{Fe}_3\text{O}_4@\text{Sal}@\text{Cu}$ [16], L-proline [17], and various types of ionic liquids [18].

Despite this, some techniques come with drawbacks, including prolonged reaction durations, intensive reaction conditions, and the utilization of toxic and non-reusable catalysts. As a result of these constraints, the development of effective and recyclable catalysts displaying elevated catalytic activity from the metal-organic frameworks (MOFs) category is still necessary to prepare chromenes rapidly. MOFs, known for their elevated specific surface areas, customized pore sizes, and crystalline structures, have emerged as intriguing hybrid materials for host-guest interactions [19]. MOFs provide advantages such as facile product separation, selectivity, and control over catalyst interaction time. However, heterogeneous catalysis presents certain disadvantages such as catalyst deactivation, particle fouling, removal of catalytic material due to the generation of volatile compounds, and the aggregation of catalyst crystallites. Zeolitic imidazole frameworks (ZIFs), a subset of MOFs comprising imidazole linkers and Zn^{2+} ions, have demonstrated significant progress in terms of unique structures, improved functionality, expanded pore size ranges, and catalytic properties [20-23]. Notably, ZIF-8, consisting of Zn^{2+} ions and 2-methylimidazolate as a linker, stands out as a prominent member of the ZIF family [24]. Although there is a previous report on the synthesis of chromene derivatives by condensing 4-coumarinol, hydroxynaphthoquinone, and aryl aldehydes, this preparation procedure was a long process and produced moderate results [25].

In the course of our investigation into innovative pathways for heterocyclic synthesis [26-28], we suggested wean effective solvent-free approach to synthesize chromene derivatives. This method

utilizes zeolitic imidazolate-zinc metal-organic framework (ZIF-8) as An eco-friendly and reusable catalyst [29] in a multicomponent condensation reaction that includes 4-coumarinol, hydroxynaphthoquinone, and aryl aldehydes (Scheme 1).



Scheme 1. Synthesis of chromene derivatives.

Experimental and computational

Materials and instruments

The experiments utilized commercially acquired chemicals without undergoing further purification. The identified products were confirmed by cross-referencing their IR and ^1H NMR data, as well as their melting points, with the corresponding information provided in literature references. The reaction progress was monitored by thin-layer chromatography (TLC) using silica gel plates (SILG/UV 254 and 365). The IR spectra were recorded using a Perkin Elmer model 10.03.06 IR spectrophotometer. ^1H and ^{13}C NMR spectra were captured using a Bruker DRX-300 AVANCE instrument at frequencies of 500 MHz and 75.4 MHz, respectively. A capillary melting point apparatus was used to determine melting points without additional adjustments.

Preparation of the ZIF-8 catalyst

ZIF-8 was generated through the methodology outlined by Zhiping Lai and colleagues in an entirely aqueous solution at ambient temperature [30]. So, it was prepared with a specific molar ratio of Zn^{2+} : 2-MeIm: H_2O = 1:70:1238 for this study. To begin the synthesis, 4mL of distilled water was used to dissolve 3.76g (14.7 mmol) of zinc dinitrate hexahydrate ($\text{Zn}(\text{NO}_3)_2 \cdot 6\text{H}_2\text{O}$). Subsequently, a magnetic stirring was employed to prepare a solution consisting of 2-methylimidazole (0.43g, 11.6 mmol) in 30-40 mL of deionized water (DI) until fully dissolved. Then, 6 mL of dimethyl sulfoxide (DMSO) was added.

Following this, the solution of zinc nitrate was introduced into the linker solution, leading to the swift development of a milky white solution. After stirring the synthesis mixture for 5 minutes, it underwent centrifugation at 14,000 rpm for 15 minutes to eliminate any unreacted species. The sedimented output was subsequently washed to enhance the removal of impurities. Ultimately, the prepared ZIF-8 underwent a 24-hour drying process at 65 °C to achieve the desired material.

Common protocol for synthesizing chromene derivatives (4a–4m)

A blend of aryl aldehyde, hydroxynaphthoquinone, and 4-Coumarinol (1 mmol of each) was amalgamated with ZIF-8 (0.005 g) at 100°C for 15-30 minutes without solvents.

Upon concluding the reaction, as verified by TLC monitoring, the reaction mixture underwent cooling to room temperature, and 15 mL of dichloromethane was added. The mixture was then stirred for an additional 15 minutes to dissolve the product in dichloromethane. After the filtration of the catalyst, the solvent was evaporated, and the residual substance underwent recrystallization in ethanol, resulting in the isolation of the pure product. The identification of Compounds **4a–4h**, previously documented, involved assessing their melting points and employing thin-layer chromatography (TLC) along with IR and ¹H NMR spectra as follows:

13-phenyl-12H,14H-benzo[g]chromeno[2,3-b]chromene-7,12,14(13H)-trione (4a)

Yellow solid; m.p. 300-302 °C. FT-IR (KBr) (ν_{\max}/cm): 3081, 1726, 1669, 1380, 1233. cm^{-1} . ¹H NMR (500 MHz, DMSO-*d*₆) δ : 5.05 (1 H, s, CH), 7.10-8.01 (12 H, m, 12 CH_{arom}), 8.19 (1 H, d, *J* = 7.9 Hz, CH_{arom}) ppm.

13-(4-chlorophenyl)-12H, 14H-benzo[g]chromeno[2,3-b]chromene-7,12,14(13H)-trione (4b)

Pale yellow solid; m.p. 322-324 °C. FT-IR (KBr) (ν_{\max}/cm): 3043, 1721, 1666, 1382, 1239 cm^{-1} . ¹H NMR (500 MHz, DMSO-*d*₆) δ : 5.06 (1 H, s, CH), 7.01 (2 H, d, *J* = 7.5 Hz, 2 CH_{arom}), 7.19 (2 H, d, *J* = 7.5 Hz, 2 CH_{arom}) 7.21-7.98 (7 H, m, 7 CH_{arom}), 8.05 (1 H, d, *J* = 7.9 Hz, CH_{arom}) ppm.

13-(4-nitrophenyl)-12H, 14H-benzo[g]chromeno[2,3-b]chromene-7,12,14(13H)-trione (4c)

Orange solid; m.p. 342-344 °C. FT-IR (KBr) (ν_{\max}/cm): 3072, 1716, 1665, 1382, 1239. cm^{-1} . ¹H NMR (500 MHz, DMSO-*d*₆) δ : 5.11 (1 H, s, CH), 7.06-7.92 (9 H, m, 9 CH_{arom}), 7.99 (1 H, d, *J* = 7.8 Hz, CH_{arom}), 8.26 (2 H, d, *J* = 7.9 Hz, 2 CH_{arom}) ppm.

13-(4-bromophenyl)-12H, 14H-benzo[g]chromeno[2,3-b]chromene-7,12,14(13H)-trione (4d)

Yellow solid; m.p. 326-328 °C. FT-IR (KBr) (ν_{\max}/cm): 3073, 1709, 1664, 1382, 1243 cm^{-1} . ^1H NMR (500 MHz, $\text{DMSO-}d_6$) δ : 5.03 (s, 1 H, CH), 7.25-7.80 (9 H, m, 9 CH_{arom}), 7.82 (2 H, d, $J = 7.8$ Hz, 2 CH_{arom}), 8.08 (1 H, d, $J = 7.9$ Hz, CH_{arom}) ppm.

13-(p-tolyl)-12H, 14H-benzo[g]chromeno[2,3-b]chromene-7,12,14(13H)-trione (4e)

Yellow solid; m.p. 305-307 °C. FT-IR (KBr) (ν_{\max}/cm): 3073, 1709, 1664, 1382, 1243 cm^{-1} . ^1H NMR (500 MHz, $\text{DMSO-}d_6$) δ : 2.42 (3 H, s, CH_3), 4.99 (1 H, s, CH), 7.02 (2 H, d, $J = 7.4$ Hz, 2 CH_{arom}), 7.10 (2 H, d, $J = 7.4$ Hz, 2 CH_{arom}), 7.20-7.78 (7 H, m, 7 CH_{arom}), 7.98 (1 H, d, $J = 7.9$ Hz, CH_{arom}) ppm

13-(4-methoxyphenyl)-12H, 14H-benzo[g]chromeno[2,3-b]chromene-7,12,14(13H)-trione (4f)

Yellow solid; m.p. 281-283 °C. FT-IR (KBr) (ν_{\max}/cm): 3083, 1734, 1654, 1379, 1243 cm^{-1} . ^1H NMR (500 MHz, $\text{DMSO-}d_6$) δ : 3.88 (3 H, s, OCH_3), 5.12 (1 H, s, CH), 6.90 (2 H, d, $J = 7.5$ Hz, 2 CH_{arom}), 7.15 (2 H, d, $J = 7.4$ Hz, 2 CH_{arom}), 7.24-7.76 (7 H, m, 7 CH_{arom}), 8.01 (1 H, d, $J = 7.9$ Hz, CH_{arom}) ppm.

13-(3-nitrophenyl)-12H, 14H-benzo[g]chromeno[2,3-b]chromene-7,12,14(13H)-trione (4g)

Yellow solid; m.p. 340-341°C. FT-IR (KBr) (ν_{\max}/cm): 3073, 1721, 1668, 1383, 1255. cm^{-1} . ^1H NMR (500 MHz, $\text{DMSO-}d_6$) δ : 5.06 (1 H, s, CH), 7.16-7.65 (9 H, m, 9 CH_{arom}), 7.94 (1 H, d, $J = 7.8$ Hz, CH_{arom}), 8.16 (1 H, d, $J = 7.9$ Hz, 1 CH_{arom}), 8.30 (1 H, s, CH_{arom}) ppm.

13-(2-chlorophenyl)-12H,14H-benzo[g]chromeno[2,3-b]chromene-7,12,14(13H)-trione (4h)

Yellow solid; m.p. 296-298 °C. FT-IR (KBr) (ν_{\max}/cm): 3078, 1726, 1657, 1555, 1382 cm^{-1} . ^1H NMR (500 MHz, $\text{DMSO-}d_6$) δ : 5.19 (1 H, s, CH), 7.18-7.91 (11 H, m, 11 CH_{arom}), 8.29 (1 H, d, $J = 7.7$ Hz, CH_{arom}) ppm.

The newly synthesized compounds **4l**, **4m** were characterized by ^{13}C NMR, ^1H NMR, IR, CHN, and Mass spectroscopy as follows:

13-(3-bromophenyl)-12H,14H-benzo[g]chromeno[2,3-b]chromene-7,12,14(13H)-trione (4l)

Yellow solid; m.p. 300-302°C. FT-IR (KBr) (ν_{\max}/cm): 3060, 1706, 1660, 1381, 1269. cm^{-1} . ^1H NMR (500 MHz, $\text{DMSO-}d_6$) δ : 5.03 (1 H, s, CH), 7.30-7.55 (9H, m, 9 CH_{arom}), 7.56 (2 H, d, $J = 7.8$ Hz, 2 CH_{arom}), 8.10 (1 H, d, $J = 7.8$ Hz, CH_{arom}) ppm. ^{13}C NMR (75 MHz, $\text{DMSO-}d_6$) = δ : 35.1 ($\text{CH}_{\text{sp}3}$), 85.1 (C), 122.6 (C), 124.5 (2 CH), 127.1 (CH), 127.6 (CH), 127.9 (2 CH), 128.3 (CH),

128.6 (CH), 128.8 (CH), 129.1 (C), 131.1 (C), 131.3 (C), 132.9 (CH), 135.3 (C), 137.9 (C), 144.3 (2CH), 151.2 (C), 153.0 (C), 170.3 (C), 176.2 (C=O), 183.0 (2 C=O) ppm. MS (EI) (m/z): 483.99 (M⁺). Anal. Calcd. for: C₂₆H₁₃BrO₅ (485.29): C 64.35, H 2.70%. Found: C 64.39, H 2.64%.

13-(2-nitrophenyl)-12H,14H-benzo[g]chromeno[2,3-b]chromene-7,12,14(13H)-trione (4m)

Pale orange solid; m.p. 282-284 °C. FT-IR (KBr) (v_{max}/cm): 3068, 1715, 1667, 1526, 1352 cm⁻¹. ¹H NMR (500 MHz, DMSO-*d*₆) δ: 5.10 (1 H, s, CH), 7.30 (2 H, t, *J* = 7.4 Hz, 2 CH_{arom}), 7.37-7.51 (6 H, m, 6 CH_{arom}), 7.63 (1 H, t, *J* = 7.5 Hz, CH_{arom}), 7.78 (1 H, t, *J* = 7.5 Hz, CH_{arom}), 7.92 (1 H, d, *J* = 7.9 Hz, CH_{arom}), 7.99 (1 H, d, *J* = 7.7 Hz, CH_{arom}) ppm. ¹³C NMR (75 MHz, DMSO-*d*₆) δ: 35.1 (CH_{sp3}), 86.3 (C), 126.0 (C), 127.2 (CH), 127.4 (CH), 128.2 (2 CH), 128.7 (CH), 128.9 (CH), 129.1 (CH), 129.5 (2 CH), 130.6 (2 CH), 131.3 (CH), 132.2 (C), 134.0 (C), 137.8 (C), 142.7 (C), 145.8 (C), 151.1 (C), 152.7 (C), 166.1 (C), 174.6 (C=O), 187.0 (2 C=O) ppm. MS (EI) (m/z): 451.07 (M⁺). Anal. Calcd. for: C₂₆H₁₃NO₇ (451.39): C 69.18, H 2.90, N 3.10%. Found: C 69.29, H 2.87, N 3.07%.

Computational Details

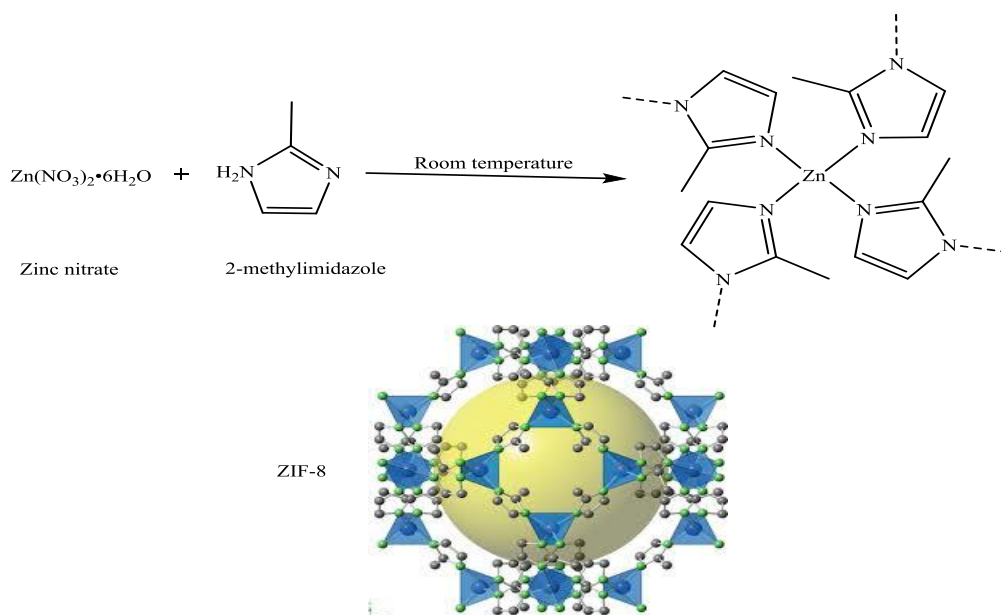
The standard Gaussian'09 programs [31] were used to carry out all calculations. The geometries of 4g, 4h, 4l, and 4m chromenes that have two conformers were fully optimized using density functional theory (DFT). The traditional hybrid exchange-correlation Becke, three-parameter, Lee–Yang–Parr (B3LYP) [32, 33] functional with 6-31G(d,p) [34] basis set were applied. Vibrational frequencies and thermodynamic properties were calculated at the same level of theory to characterize the stationary points. No imaginary frequencies were observed using GaussView [35] and Chemcraft [36] software.

Results and discussion

ZIF-8 framework and composition:

The synthesis of ZIF-8 was carried out according to the established procedure in the literature [30]. As illustrated in Scheme 2, the structure of ZIF-8 comprises zinc atoms coordinated to nitrogen atoms through 2-methylimidazolate (MeIM) linkers, resulting in a nanoporous framework. This framework is characterized by Zn₄N tetrahedral clusters that form four-, six-, eight-, and twelve-membered rings.

The catalyst was characterized using several analytical techniques, including scanning electron microscopy (SEM), X-ray diffraction (XRD), Fourier-transform infrared spectroscopy (FT-IR), energy-dispersive X-ray spectroscopy (EDX), and Brunauer-Emmett-Teller (BET) analysis.



Scheme 2. Preparation process of the ZIF-8.

Scanning electron microscopy (SEM) proves to be an invaluable tool in the examination of size distribution, particle shape, and porosity. By employing this technique (Figure 1), an assessment of the morphology and particle size of ZIF-8 was conducted.

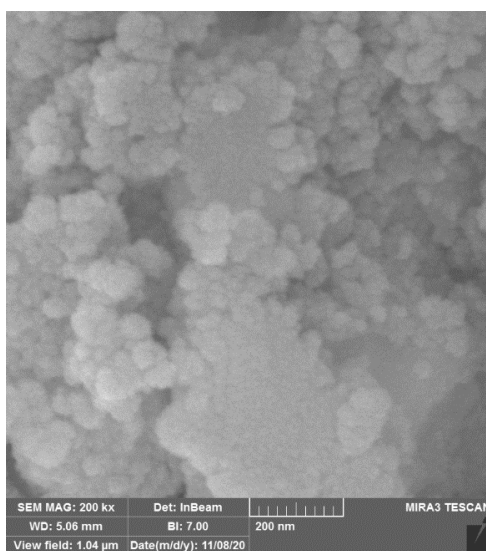


Figure 1. SEM image of the ZIF-8.

Energy-dispersive X-ray spectroscopy (EDX) experiments were conducted to assess the purity and stoichiometry of ZIF-8. Figure 2 displays the elemental composition of the MOF catalyst, confirming the presence of key constituents-carbon (C), nitrogen (N), oxygen (O), and zinc (Zn)-within the synthesized structure.

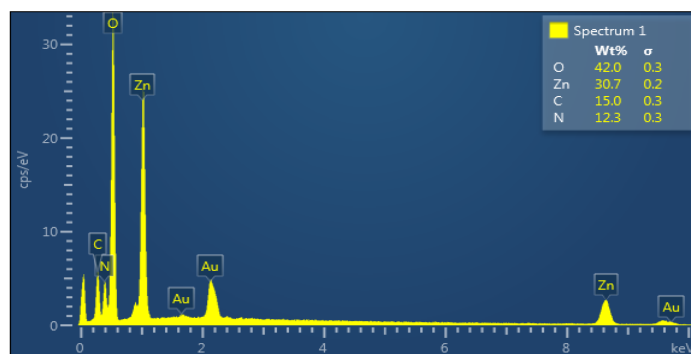


Figure 2. EDX spectra of the ZIF-8.

Additionally, elemental mapping of ZIF-8 was performed using EDX analysis (Figure 3). The uniform distribution of these elements strongly indicates a composition free of impurities in the fabricated nanocatalyst. Specifically, the distributions of C (Figure 3a), N (Figure 3b), O (Figure 3c), and Zn (Figure 3d) not only demonstrate high purity but also reveal a consistent arrangement throughout the ZIF-8 framework. Finally, Figure 3e illustrates this uniform distribution, highlighting the structural integrity of the catalyst.

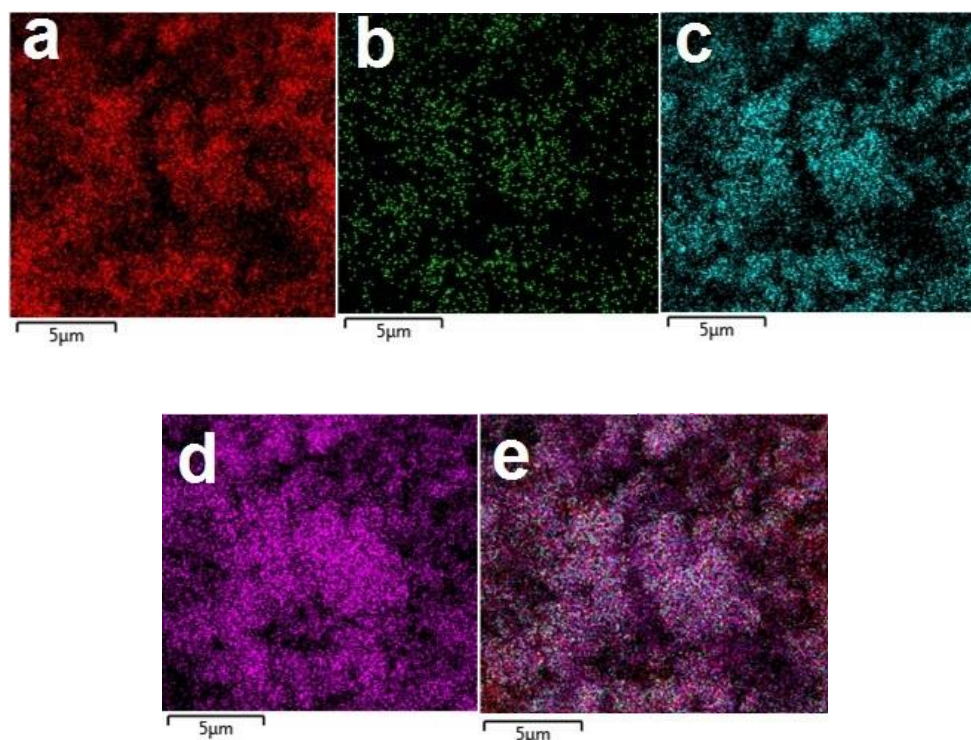


Figure 3. EDX elemental mapping of the ZIF-8.

Figure 4 presents the X-ray diffraction (XRD) pattern of the synthesized catalyst. The distinct peaks observed in the pattern closely align with those previously reported for ZIF-8. These clearly defined peaks indicate a high degree of crystallinity in the synthesized MOFs. The X-ray diffraction (XRD) pattern of ZIF-8 typically exhibits several distinct peaks within the 2θ range of 10 to 50°. Notable peaks include one at approximately 10.4°, which corresponds to the (200) plane, followed by a peak

at 12.7° associated with the (211) plane. The peak at 14.4° is attributed to the (220) plane, while the peak at 16.5° corresponds to the (310) plane. Additionally, a peak at 18.3° is linked to the (321) plane. Other significant peaks include one at 22.5° for the (222) plane, 25.0° for the (400) plane, and 26.9° for the (420) plane. Further peaks are observed at 29.5° , corresponding to the (511) plane, and at 34.0° for the (600) plane, with an additional peak at 38.0° linked to the (620) plane. These peaks indicate the crystalline nature of ZIF-8 and confirm its structural integrity. The presence of sharp and well-defined peaks suggests a high degree of crystallinity. The specific positions of these peaks may vary slightly based on synthesis conditions, sample preparation, and the specific XRD equipment used. These findings confirm the successful synthesis of the targeted MOF and affirm its structural purity, with no detectable impurities present.

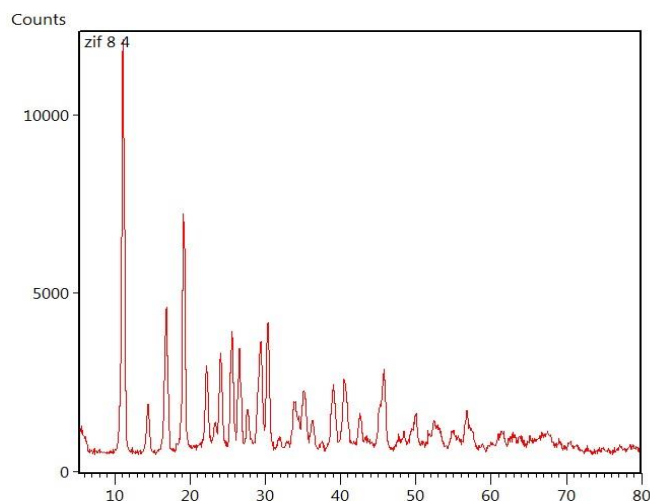


Figure 4. XRD pattern of the ZIF-8.

Figure 5 presents the FT-IR spectra of ZIF-8. A prominent peak at 430 cm^{-1} indicates Zn-N stretching, reflecting the interaction between zinc and nitrogen atoms in the 2-methylimidazole component of the ZIF-8 structure during synthesis. Within the range of 1350 to 900 cm^{-1} , several spectral bands were observed, likely associated with the in-plane bending of the aromatic ring. Additionally, bands at 763 and 692 cm^{-1} correspond to the sp^2 C-H bending of the aromatic portion of the ring. The peak at 1596 cm^{-1} is attributed to the C=N bond of the imidazole ring. In the spectral range of 3500 – 3200 cm^{-1} , N-H bond stretching is observed, along with two smaller peaks at 3135 cm^{-1} and between 3000 – 2850 cm^{-1} . These smaller peaks are likely the result of vibrational modes of C-H stretching in both the imidazole ring and the methyl group.

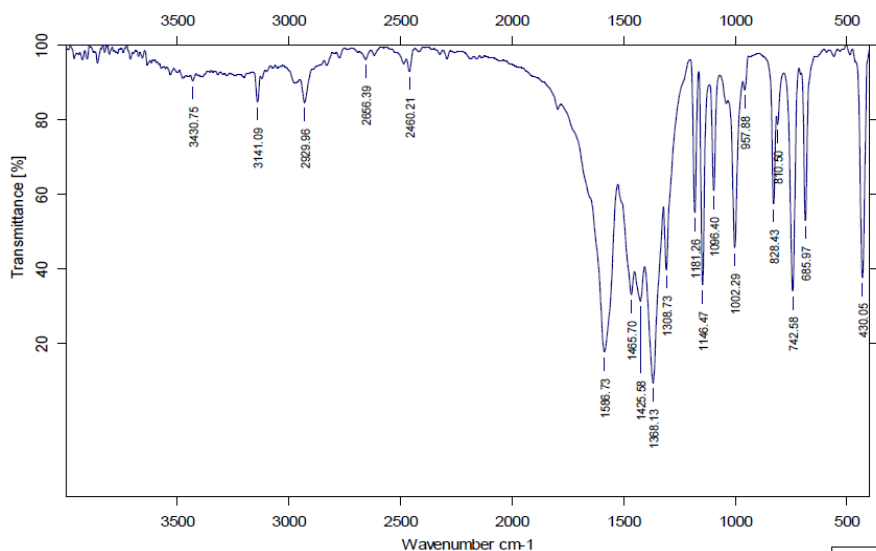


Figure 5. FT-IR spectrum of the ZIF-8.

In adsorption applications, the specific surface area and pore volume of metal-organic frameworks (MOFs) are critical factors. The pore size distribution and BET surface area of ZIF-8 were determined using nitrogen adsorption/desorption isotherms at 77 K, as illustrated in Figure 6. The results confirm that ZIF-8 exhibits a microporous structure. The calculated BET surface area and total pore volume of the synthesized ZIF-8 catalyst are 1700 m²/g and 0.664 cm³/g, respectively. This data highlights the effective adsorption properties of the prepared ZIF-8 material, emphasizing its potential for various applications.

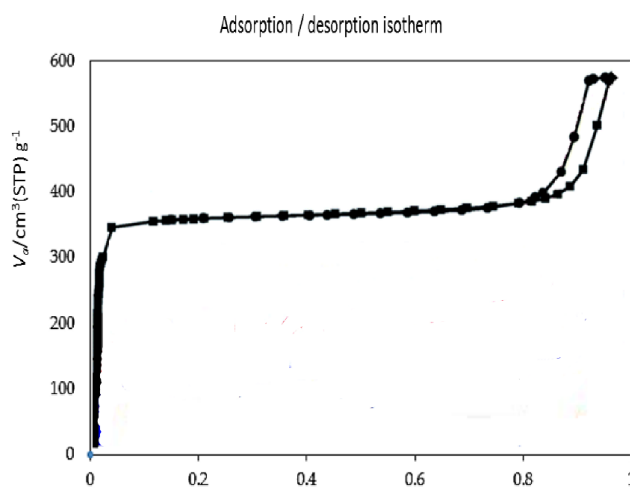


Figure 6. The N₂ adsorption-desorption isotherms at 77 K of the ZIF-8

Catalytic activity

In the initial investigations aimed at optimizing reaction conditions, a model reaction involving 2-hydroxynaphthalene-1,4-dione, 4-nitrobenzaldehyde, hydroxynaphthoquinone, and 4-Coumarinol was selected. The synthesis of compound 4c in a one-pot reaction was performed without any solvent at 100 °C. The optimization of the reaction parameters for synthesizing chromene derivatives involved exploring different solvents, catalysts, and temperatures. To achieve this, a model reaction was conducted with the different quantities of ZIF-8. Based on the findings in Table 1, the ideal quantity of ZIF-8 was determined to be 0.005 g.

Upon increasing this quantity, no changes were observed in the reaction yields or time. As a result, the output yield decreased when the catalyst amount was reduced. Hence, the optimal level of ZIF-8 in the model reaction was determined as 0.005 g (Table 1). Further experiments with 0.005 g of ZIF-8 at various temperatures ranging from 50°C to 110°C resulted in prolonged reaction durations and reduced yields.

Table 1. The impact of catalyst quantities and temperature on the synthesis of 4c

Entry	Catalyst (g)	Temperature (°C)	Time/min.	Yield (%) ^a
1	No catalyst	100	360	No reaction
2	0.001	100	60	70
3	0.003	100	60	80
4	0.005	100	15	98
5	0.007	100	30	97
6	0.005	50	30	78
7	0.005	70	30	83
8	0.005	90	30	92
9	0.005	110	30	94

^a Isolated yields.

The model reaction to produce chromenes was conducted using ZIF-8 with various solvents and also in a solvent-free setup. The most favorable results were attained under solvent-free conditions, as demonstrated in Table 2 (refer to Table 2, entry 6).

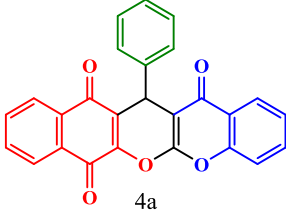
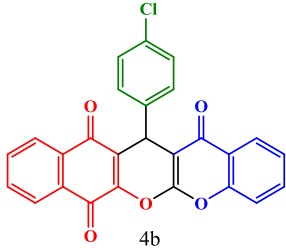
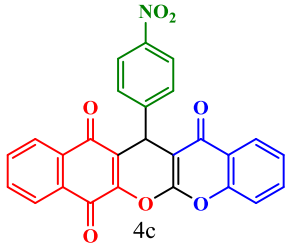
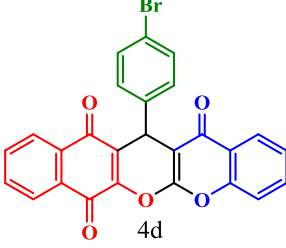
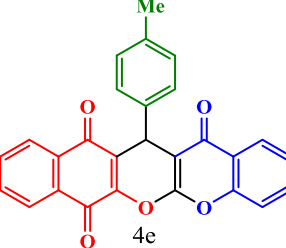
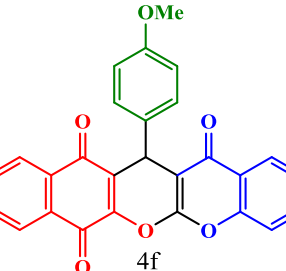
Table 2. The effect of the solvents on the synthesis of 4c.

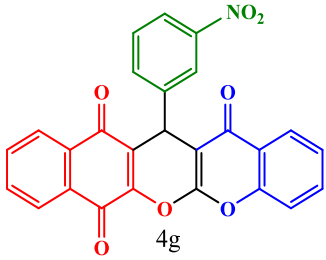
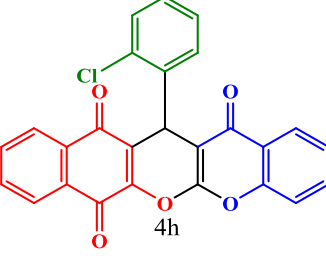
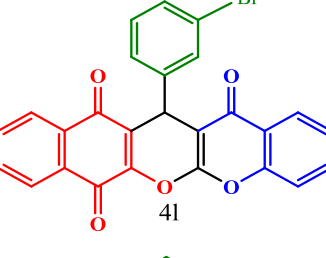
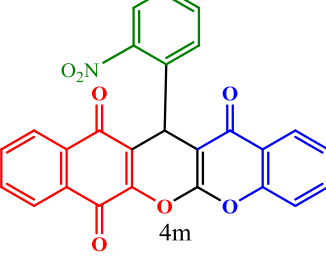
Entry	Solvents	Time/min.	Yield (%) ^a
1	H ₂ O-EtOH (reflux)	60	70
2	Toluene (reflux)	60	27
3	Dichloromethane (reflux)	60	50
4	Ethanol (reflux)	60	65
5	Acetonitrile (reflux)	60	42
6	Solvent-free	15	98

^a Isolated yields.

After the most optimal reaction conditions were determined using the ZIF-8 catalyst, other substituted aldehydes were applied in comparable three-component reactions. Throughout all the processes, ZIF-8 consistently yielded satisfactory results for the final products. The summarized findings are presented in Table 3.

Table 3. Synthesis of chromenes using the ZIF-8 as the catalyst^a

Entry	product	R	Yield (%) ^b	M.P.(°C)	M.P.(°C) [16]
1	 4a	C ₆ H ₅	91	300-302	301-303
2	 4b	4-Cl-C ₆ H ₄	96	322-324	323-325
3	 4c	4-NO ₂ -C ₆ H ₄ ^d	98 ^d	342-344	341-343
4	 4d	4-Br-C ₆ H ₄	93	326-328	328-330
5	 4e	4-Me-C ₆ H ₄	90	305-307	303-305
6	 4f	4-OMe-C ₆ H ₄	88	281-283	281-283

7		3-NO ₂ -C ₆ H ₄	95	340-341	339-341
8		2-Cl-C ₆ H ₄	91	296-298	295-297
9		3-Br-C ₆ H ₄	93	300-302 ^c	-----
10		2-NO ₂ -C ₆ H ₄	92	282-284 ^c	-----

^aReaction conditions: 2-hydroxynaphthalene-1,4-dione (1 mmol), 4-hydroxycoumarin (1 mmol) and aromatic aldehydes (1 mmol) in the presence of ZIF-8 were heated at 100°C under solvent-free conditions.

^bYield obtained after 15-30 min.

^cNovel compounds.

^d**4c**, yield 98% under the influence of the ZIF-8 for the first time, 96% in the second run, and 95% in the third run with the recycled catalyst.

The possibility of reusing ZIF-8 as a catalyst in the synthesis of **4c** was explored (refer to Table 3, entry 3). Upon completion of the reaction, the catalyst was effortlessly separated from the mixture through rapid centrifugation, enabling its convenient reuse in subsequent processes. Although ZIF-8 showed a slight reduction in catalytic activity after three runs, it remains a valuable and recyclable catalyst.

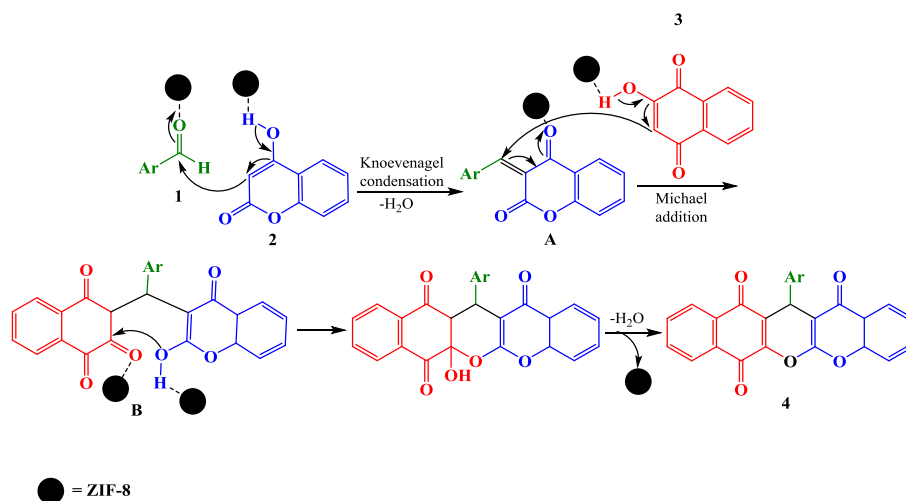
To highlight the importance of this investigation, the catalytic efficiency of ZIF-8 was compared with the sole previously reported catalyst for chromene synthesis [25] (Table 4). The comparison revealed that our catalyst yielded higher product yields within significantly shorter reaction periods. This finding further underscores the efficacy of utilizing ZIF-8 as a catalyst in chromene synthesis.

Table 4. The ZIF₈ catalyzed the synthesis of chromenes **4c**, compared to Fe₃O₄-IL MNPs, which is the only catalyst reported in the literature^a.

Entry	Catalyst	Conditions	Time/ Yield (%)	Reference
1	Fe ₃ O ₄ -IL MNPs	H ₂ O-EtOH (1:1)	4 h/ 92	16
2	ZIF-8	Solvent-free/ 100 °C	15 min/ 98	This work

^aBased on the three-component reaction of 4-nitrobenzaldehyde, 4-hydroxycoumarin and 2-hydroxynaphthalene-1,4-dione.

Scheme 3 illustrates one of the proposed synthesis routes for chromene derivatives using ZIF-8 as a heterogeneous catalyst. ZIF-8 functions as a catalyst with dual capabilities, encompassing both basic and acidic sites. The Lewis acid properties are ascribed to the Zn²⁺ ions, whereas its alkaline properties are derived from the basic imidazole groups. The mechanism involves named reactions such as Knoevenagel and Michael addition, along with intramolecular cyclization and subsequent dehydration stages. Through Knoevenagel reaction between 4-Coumarinol **1** and aldehyde **2**, a conjugated electron-deficient enone **A** is formed. Subsequently, intermediate **B** was produced through the Michael addition reaction between the α , β -unsaturated carbonyl compound (intermediate **A**) and hydroxynaphthoquinone **3**. This intermediate then undergoes cyclodehydration in the presence of ZIF-8 to yield the desired chromene derivatives. The nanocomposite catalyst based on ZIF-8, with surface sites exhibiting both acidic and basic characteristics, plays a pivotal role in facilitating the reaction. It achieves this by extracting acidic protons and activating the carbonyl group for nucleophilic attack.

**Scheme 3.** A plausible mechanism for the ZIF-8-catalyzed synthesis of chromene derivatives.

Conformational analysis

Figure 7 shows the structure of **4g**, **4h**, **4l**, and **4m** chromenes and their interconversion-conformers (**4g'**, **4h'**, **4l'** and **4m'**) which have been optimized using B3LYP functional with 6-31G(d,p) basis

set. Table 5 lists the thermodynamic properties: ΔH° , ΔS_{th} , ΔG° , and K_{eq} for the interconversion of chromenes' conformers at 298 K and 1 atm in the gas phase and DMSO solvent.

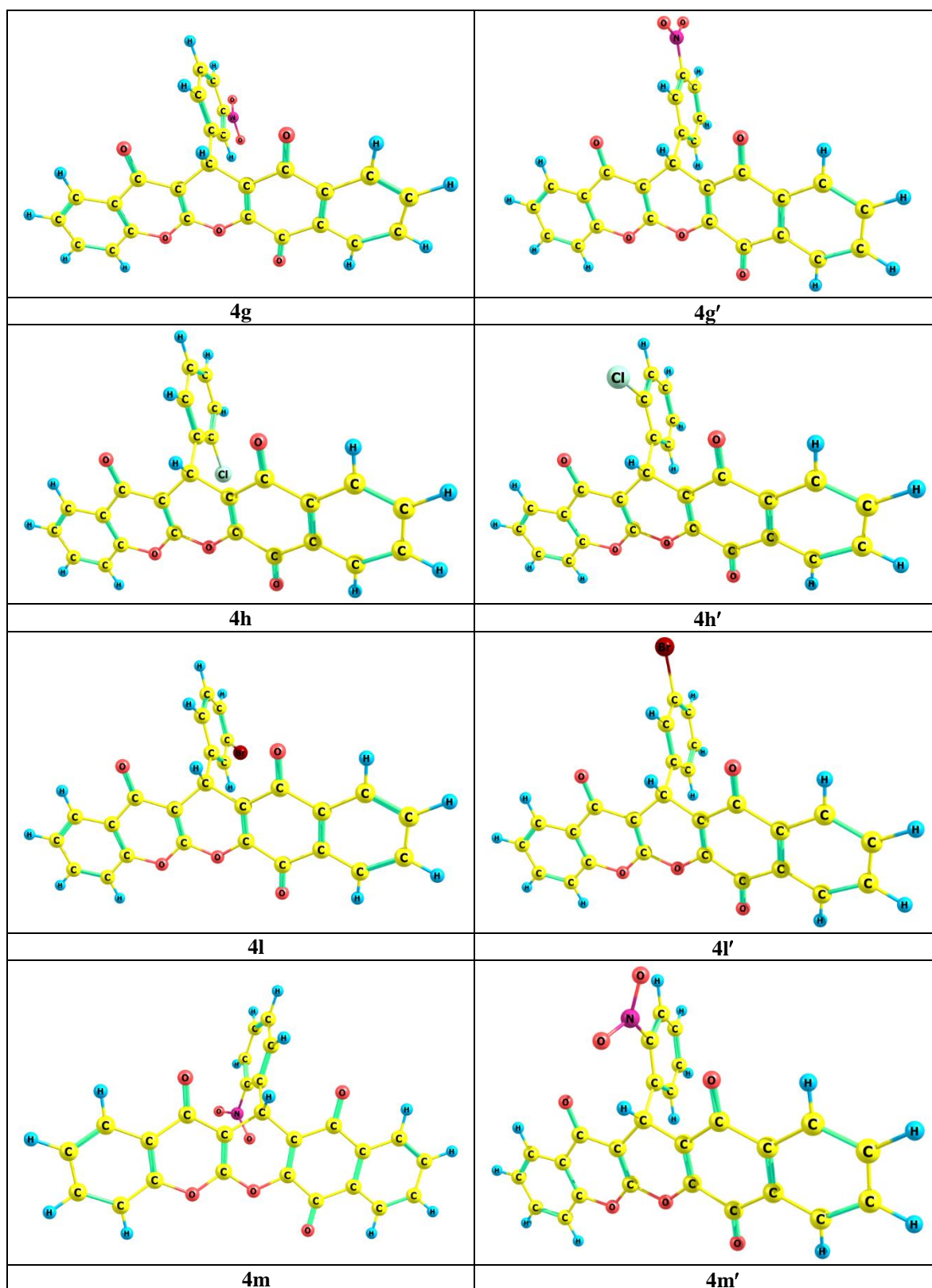


Figure 7. The optimized structure of 4g, 4h, 4l and 4m chromenes and their conformers (4g', 4h', 4l' and 4m') using B3LYP/6-31G(d,p) level of theory.

Table 5. Thermodynamic properties of the conversion of chromenes' conformers at 298 K and 1 atm in the gas phase and DMSO solvent using B3LYP/6-31G(d,p) level of theory.

	ΔH° (kcal/mol)	ΔS_{th} (cal/mol.K)	ΔG° (kcal/mol)	K_{eq}
4g \rightarrow 4g'	0.824 (0.057)	-0.651 (-0.268)	1.018 (0.136)	0.179 (0.794)
4h \rightarrow 4h'	0.862 (-0.584)	1.178 (0.825)	0.511 (-0.831)	0.422 (4.063)
4l \rightarrow 4l'	0.319 (-0.017)	0.787 (1.027)	0.084 (-0.323)	0.867 (1.726)
4m \rightarrow 4m'	0.178 (-1.808)	1.775 (0.488)	-0.351 (-1.953)	1.807 (27.036)

The thermodynamic properties in the solvent phase are in parentheses.

The lowest standard enthalpy (ΔH°) is related to the conversion of conformer 4m \rightarrow 4m' (0.178 kcal/mol), while the highest is related to the conversion of conformer 4h \rightarrow 4h' (0.862 kcal/mol) in the gas phase. Although the DMSO solvent has the lowest enthalpy value associated with the conversion of conformer 4m \rightarrow 4m' (-1.808 kcal/mol), the highest value is related to 4g \rightarrow 4g' (0.057 kcal/mol).

As can be seen, DMSO solvent, unlike the gaseous environment, stabilizes the second form of conformers, and the highest stability is seen in the conformer 4m'. No particular trend can be seen regarding the entropy of conformers. But regarding the Gibbs free energy of conformer transformation, the highest one (1.018 kcal/mol in gaseous phase and 0.136 kcal/mol in DMSO phase) is related to 4g \rightarrow 4g' and the lowest one (-0.351 kcal/mol in gaseous phase and -1.953 kcal/mol in DMSO phase) is related to 4m \rightarrow 4m'. The results show that the solvent environment has caused the second form of the conformer to become more stable and the increase in stability can be seen in the 4m' > 4l' > 4h' > 4g' conformers respectively. These results are also confirmed by the equilibrium constant of the conversion of conformers, which is mostly the equilibrium constant in DMSO solvent (27.04) related to the conversion 4m \rightarrow 4m'.

Conclusion

In conclusion, The effective production of chromenes has been successfully presented using a thermal, solvent-free, eco-friendly approach, with ZIF-8 utilized as a catalyst. The final products resulted from a three-component reaction that involved hydroxynaphthoquinone, 4-Coumarinol, and aryl aldehydes, with ZIF-8 acting as a reusable catalyst, conducted without any solvent. Notably, this method offers numerous benefits, including neutral reaction conditions, the use of starting materials without activation or modification, mild reaction conditions, a brief reaction time, straightforward work-up, reusability of the catalyst, and high yields of biologically active products.

In conformational analysis of 4g \leftrightarrow 4g', 4h \leftrightarrow 4h', 4l \leftrightarrow 4l' and 4m \leftrightarrow 4m', the results show that the solvent environment has caused the second form of the conformer that has less intramolecular interaction to become more stable. The increase of stability can be seen in the 4m' > 4l' > 4h' > 4g' conformers respectively. The maximum value of the equilibrium constant in DMSO solvent i.e: 27.04 is related to the conversion of 4m \rightarrow 4m'.

Acknowledgments

The authors convey their appreciation for the assistance provided for this research from the Islamic Azad University, Yadegar-e-Imam Khomeini (RAH) Shahre-rey Branch, Tehran, Iran.

References

1. Dömling A, Ugi I. Multicomponent reactions with isocyanides. *Angewandte Chemie International Edition*. 2000; 39(18): 3168-3210.
2. (a) Dömling A. Recent developments in isocyanide based multicomponent reactions in applied chemistry. *Chemical reviews*. 2006; 106 (1): 17-89.
(b) Ghasemzadeh MA, Mirhosseini-Eshkevari B, Tavakoli M, Zamani F. Metal–organic frameworks: advanced tools for multicomponent reactions. *Green Chemistry*. 2020; 22(21): 7265-7300.
3. Khafagy MM, Abd El-Wahab AH., Eid FA, El-Agrody AM. Synthesis of halogen derivatives of benzo [h] chromene and benzo [a] anthracene with promising antimicrobial activities. *Il Farmaco*. 2002; 57(9): 715-722.
4. Smith PW, Sollis SL, Howes PD, Cherry PC, Starkey ID, Copley KN, et al. Dihydropyranocarboxamides related to zanamivir: A new series of inhibitors of influenza virus sialidases. 1. Discovery, synthesis, biological activity, and structure– activity relationships of 4-guanidino-and 4-amino-4 H-pyran-6-carboxamides. *Journal of Medicinal Chemistry*. 1998; 41(6): 787-797.
5. de Andrade-Neto VF, Goulart MO., da Silva Filho JF, da Silva MJ, Pinto M do CF., Pinto A V, et al. Antimalarial activity of phenazines from lapachol, β -lapachone and its derivatives against *Plasmodium falciparum* in vitro and *Plasmodium berghei* in vivo. *Bioorganic & medicinal chemistry letters*. 2004;14(5): 1145-1149.
6. Anderson DR, Hegde S, Reinhard E, Gomez L, Vernier WF, Lee L, et al. Aminocyanopyridine inhibitors of mitogen activated protein kinase-activated protein kinase 2 (MK-2). *Bioorganic & Medicinal Chemistry Letters*. 2005; 15(6): 1587-1590.
7. Pérez-Sacau E, Estévez-Braun A, Ravelo ÁG, Gutiérrez Yapu D, Giménez Turba A. Antiplasmodial Activity of Naphthoquinones Related to Lapachol and β -Lapachone. *Chemistry & Biodiversity*. 2005; 2(2): 264-274.
8. Ellis GP. In the chemistry of heterocyclic compounds: chromenes, chromanones, and chromones, A. Weissberger, E. C. Taylor Eds., New York, John Wiley, 1977.

9. Sofan MA, El-Taweel FM, Elagamey AGA, Elnagdi MH. Studies on cinnamionitriles: The reaction of cinnamionitriles with cyclopentanone. *Liebigs Annalen der Chemie*. 1989;1989(9): 935-936.
10. Balou J, Khalilzadeh MA, Zareyee D. An efficient and reusable nano catalyst for the synthesis of benzoxanthene and chromene derivatives. *Scientific Reports*. 2019; 9(1): 3605.
11. Ghavidel H, Mirza B, Soleimani-Amiri S. A novel efficient, and recoverable basic Fe₃O₄@ C nano-catalyst for green synthesis of 4 H-chromenes in water via one-pot three component reactions. *Polycyclic Aromatic Compounds*. 2021; 41(3): 604-625.
12. Ghashang M. ZnAl₂O₄-Bi₂O₃ composite nano-powder as an efficient catalyst for the multi-component, one-pot, aqueous media preparation of novel 4 H-chromene-3-carbonitriles. *Research on Chemical Intermediates*. 2016; 42(5): 4191-4205.
13. Bahrami S, Hassanzadeh-Afruzi F, Maleki A. Synthesis and characterization of a novel and green rod-like magnetic ZnS/CuFe₂O₄/agar organometallic hybrid catalyst for the synthesis of biologically-active 2-amino-tetrahydro-4H-chromene-3-carbonitrile derivatives. *Applied Organometallic Chemistry*. 2020; 34(11): e5949.
14. Naeimi H, Mohammadi S. Synthesis of 1H-Isochromenes, 4H-Chromenes and Orthoaminocarbonitrile Tetrahydronaphthalenes by CaMgFe₂O₄ Base Nanocatalyst. *ChemistrySelect*. 2020; 5(8): 2627-2633.
15. Abbasi Pour S, Yazdani-Elah-Abadi A, Afradi M. Nanomagnetically modified thioglycolic acid (γ -Fe₂O₃@ SiO₂-SCH₂CO₂H): Efficient and reusable green catalyst for the one-pot domino synthesis of spiro [benzo [a] benzo [6, 7] chromeno [2, 3-c] phenazine] and benzo [a] benzo [6, 7] chromeno [2, 3-c] phenazines. *Applied Organometallic Chemistry*. 2017; 31(11): e3791.
16. Ferdousian R, Behbahani FK, Mohtat B. Synthesis and characterization of Fe₃O₄@ Sal@ Cu as a novel, efficient and heterogeneous catalyst and its application in the synthesis of 2-amino-4H-chromenes. *Molecular Diversity*. 2022; 26(6): 3295-3307.
17. Daloe TS, Behbahani FK. A Green Route for the Synthesis of 2-Amino-5, 10-dioxo-4-aryl-5, 10-dihydro-4H-benzo [g] chromene-3-carbonitriles Using L-Proline as a Basic Organocatalyst. *Polycyclic Aromatic Compounds*. 2022; 42(3): 681-689.
18. Chatterjee R, Bhukta S, Dandela R. Ionic liquid-assisted synthesis of 2-amino-3-cyano-4 H-chromenes: A sustainable overview. *Journal of Heterocyclic Chemistry*. 2022; 59(4): 633-654.
19. (a) Ghose AK, Viswanadhan VN, Wendoloski JJ. A knowledge-based approach in designing combinatorial or medicinal chemistry libraries for drug discovery. 1. A qualitative and quantitative characterization of known drug databases. *Journal of combinatorial chemistry*. 1999; 1(1): 55-68.

- (b) Yang Q, Xu Q, Jian, HL. Metal–organic frameworks meet metal nanoparticles: synergistic effect for enhanced catalysis. *Chemical Society Reviews*. 2017; 46(15): 4774-4808.
- (c) Wang C, Liu D, Lin W. Metal–organic frameworks as a tunable platform for designing functional molecular materials. *Journal of the American Chemical Society*. 2013; 135(36): 13222-13234.
- (d) Hu M-L, Safarifard V, Doustkhah E, Rostamnia S, Morsali A, Nouruzi N, et al. Taking organic reactions over metal-organic frameworks as heterogeneous catalysis. *Microporous and mesoporous materials*. 2018; 256(36): 111-127.
20. Augustine RL, O'Leary ST. Heterogeneous catalysis in organic chemistry. Part 10. Effect of the catalyst support on the regiochemistry of the heck arylation reaction. *Journal of Molecular Catalysis A: Chemical*. 1995; 95(3): 277-285.
21. Cremer E. The compensation effect in heterogeneous catalysis. In *Advances in Catalysis*. Academic Press. 1955; 7:75-91.
22. Chen B, Yang Z, Zhu Y, Xia Y. Zeolitic imidazolate framework materials: recent progress in synthesis and applications. *Journal of Materials Chemistry A*. 2014; 2(40): 16811-16831.
23. (a) Park KS, Ni Z, Côté AP, Choi JY, Huang R, Uribe-Romo FJ, et al. Exceptional chemical and thermal stability of zeolitic imidazolate frameworks. *Proceedings of the National Academy of Sciences*. 2006; 103(27): 10186-10191.
- (b) Wu H, Zhou W, Yildirim T. Hydrogen storage in a prototypical zeolitic imidazolate framework-8. *Journal of the American Chemical Society*. 2007; 129(17): 5314-5315.
24. Chokbunpiam T, Chanajaree R, Remsungnen T, Saengsawang O, Fritzsche S, Chmelik C, Hannongbua S. N₂ in ZIF-8: Sorbate induced structural changes and self-diffusion. *Microporous and Mesoporous Materials*. 2014; 187(17): 1-6.
25. Safaei-Ghomi J, Eshteghal F, Shahbazi-Alavi H. Novel ionic liquid supported on Fe₃O₄ nanoparticles as an efficient catalyst for the synthesis of new chromenes. *Applied Organometallic Chemistry*. 2018; 32(1): e3987.
26. Shahvelayati AS, Yavari I, Delbari, AS. Formation of thiazol-2 (3H)-imines by reaction of α -amino acids, aroylisothiocyanates, and α -bromoketones in an ionic liquid. *Chinese Chemical Letters*. 2014; 25(1): 119-122.
27. Yavari I, Ghanbari MM, Shahvelayati AS, Ghazvini M. Chemoselective Synthesis of Functionalized 2, 5-Dihydro-2-thioxo-1 H-imidazoles from 5, 5-Diarylthiohydantoin and Activated Acetylenes. *Phosphorus, Sulfur, and Silicon*. 2010; 185(12): 2551-2557.

28. Shahvelayati AS, Sabbaghan M, Banihashem S. Sonochemically assisted synthesis of N-substituted pyrroles catalyzed by ZnO nanoparticles under solvent-free conditions. *Monatshefte Für Chemie-Chemical Monthly*. 2017; 148(6): 1123-1129.
29. Alibakhshi Sh, Shahvelayati AS, Sheshmani Sh, Ranjbar M, Souzangarzadeh S. Design, synthesis, and characterization of a novel Zn (II)-2-phenyl benzimidazole framework for the removal of organic dyes. *Scientific Reports* 2022; 12 (1): 12431.
30. (a) Pan Y, Liu Y, Zeng G, Zhao L, Lai Z. Rapid synthesis of zeolitic imidazolate framework-8 (ZIF-8) nanocrystals in an aqueous system. *Chemical Communications*. 2011; 47(7): 2071-2073.
- (b) Zhou X, Zhang HP, Wang GY, Yao ZG, Tang YR, Zheng SS. Zeolitic imidazolate framework as efficient heterogeneous catalyst for the synthesis of ethyl methyl carbonate. *Journal of Molecular Catalysis A: Chemical*. 2013; 366(7): 43-47.
- (c) Du Y, Chen, RZ, Yao JF, Wang HT. Facile fabrication of porous ZnO by thermal treatment of zeolitic imidazolate framework-8 and its photocatalytic activity. *Journal of Alloys and Compounds*. 2013; 551(7): 125-130.
- (d) Tran UP, Le KK, Phan NT. Expanding applications of metal-organic frameworks: zeolite imidazolate framework ZIF-8 as an efficient heterogeneous catalyst for the knoevenagel reaction. *Acs Catalysis*. 2011; 1(2): 120-127.
- (e) Zhang Y, Jia Y, Li M, Hou L. Influence of the 2-methylimidazole/zinc nitrate hexahydrate molar ratio on the synthesis of zeolitic imidazolate framework-8 crystals at room temperature. *Scientific reports*. 2018; 8(1): 9597.
31. Frisch MJ, Trucks GW, Schlegel HB, Scuseria GE, Robb MA, Cheeseman JR, Scalmani G, Barone V, Mennucci B, Petersson GA, et al. *Gaussian 09, revision A.02-SMP*, Gaussian, Inc.: Wallingford, CT, USA, 2009.
32. Becke AD. Density-functional exchange-energy approximation with correct asymptotic behavior. *Physical review A*. 1988; 38(6): 3098.
33. Lee C, Yang W, Parr RG. Development of the Colle-Salvetti correlation-energy formula into a functional of the electron density. *Physical review B*. 1988; 37(2): 785.
34. Ditchfield R, Hehre WJ, Pople JA. Self-consistent molecular-orbital methods. IX. An extended Gaussian-type basis for molecular-orbital studies of organic molecules. *The Journal of Chemical Physics*. 1971; 54(2): 724-728
35. Dennington R, Keith T, Millam J. *GaussView*; Semichem Inc. Shawnee Mission, KS; 2009.
36. Aziz S, Osman O, Elroby S, Hilal RH. Gas-phase thermal tautomerization of imidazole-acetic acid: theoretical and computational investigations. *International Journal of Molecular Sciences*. 2015;16(11): 26347-26362.